

Identification of film-based formulations that move mRNA lipid nanoparticles out of the freezer

Trang Nguyen Kieu Doan,¹ Madison M. Davis,¹ and Maria A. Croyle^{1,2}

¹College of Pharmacy, Division of Molecular Pharmaceutics and Drug Delivery, The University of Texas at Austin, Austin, TX 78712, USA; ²John R. LaMontagne Center for Infectious Disease, The University of Texas at Austin, Austin, TX 78712, USA

COVID-19 vaccines consisting of mRNA lipid nanoparticles (LNPs) encoding the severe acute respiratory syndrome coronavirus 2 (SARS-CoV-2) spike protein antigen protected millions of people from severe disease; however, they must be stored frozen prior to use. The objective of this study was to evaluate the compatibility and stability of mRNA LNPs within a polymer-based film matrix. An optimized formulation of polymer base, glycerol, surfactants, and PEGylated lipid that prevents damage to the LNP due to physical changes during the film-forming process (osmotic stress, surface tension, spatial stress, and water loss) was identified. Surfactants added to LNP stock prior to mixing with other film components contributed to this effect. Formulations prepared at pH \geq 8.5 extended transfection efficiency beyond 4 weeks at 4°C when combined with known nucleic acid stabilizers. mRNA LNPs were most stable in films when manufactured in an environment of \sim 50% relative humidity. The optimized formulation offers 16-week stability at 4°C.

INTRODUCTION

While use of lipid nanoparticles (LNPs) to deliver mRNA was first described in the late 1970s,¹ their approval in several mRNA-based vaccines during the COVID-19 pandemic brought them to the forefront of the biotech industry. Emergency use authorization from the United States Food and Drug Administration and European Medicines Agency and global distribution of the BioNTech/Pfizer and Moderna severe acute respiratory syndrome coronavirus 2 (SARS-CoV-2) mRNA vaccines provided solid evidence that the mRNA LNP platform could effectively induce expression of antigens in a manner that prevented severe disease.^{2,3} Since then, basic research and clinical trials using mRNA LNPs to express therapeutic proteins or antibodies to treat genetic, cardiovascular, and other infectious diseases as well as gene editing have risen exponentially.^{1,4}

LNPs are fatty droplets with an aqueous core that contains a series of reversed micelles that bind, protect, and deliver mRNA nucleotides (Figure S1).⁵ Several different types of lipids are commonly used to make these particles. Ionizable lipids retain a positive charge within the acidic environment of the aqueous core to form micellar networks that bind mRNA through electrostatic interactions. When they reach

physiological pH in solution or a living organism, they become neutral, making them biocompatible. In the endosome, ionizable lipids revert to their original positively charged state where they interact with anionic phospholipids to disrupt the endosomal membrane and facilitate release of intact mRNA-containing micelles into the cytoplasm.^{6,7} Neutral phospholipids and cholesterol are responsible for maintaining an organized lipid shell. Helper lipids such as distearoylphosphatidylcholine (DSPC) also contribute to endosomal escape by interacting with the endosomal membrane.⁸ Small amounts of lipids attached to polyethylene glycol (PEG) dispersed throughout the lipid phase of the particle can significantly affect particle size, surface charge, and physical stability as they have been shown to prevent aggregation, extend circulation time, and reduce particle clearance.^{1,9,10} PEG molecules on the outer shell of the particle also create a hydration shell that circumvents opsonization and partially governs particle stability. PEG can also serve as a linker for attachment of targeting molecules to limit where particles are taken up and genes expressed.¹¹

LNPs containing mRNA are generally prepared by mixing single-stranded ribonucleic acid molecules in an acidic aqueous buffer with lipids in an ethanolic solution in a microfluidic system where speed, volume ratio, and the flow pattern are highly controlled.¹² In practice, 40–80% of LNPs prepared in this manner do not contain any mRNA, while each LNP carries two to six mRNA molecules.¹³ Unencapsulated material is removed by dialysis or ultracentrifugation and particles suspended in a buffer, often phosphate-buffered saline (PBS, pH 7.4) or Tris (pH 8). Buffer selection has been shown to significantly affect the physical stability of LNPs. For example, Tris-buffered self-replicating mRNA LNPs showed larger particle size than those stored in PBS at 4°C and -20°C .¹⁴ Tris buffer was also found to minimize changes in solution pH during freezing and slow adduct formation of aldehyde

Received 19 October 2023; accepted 21 March 2024;
<https://doi.org/10.1016/j.omtn.2024.102179>.

Correspondence: Maria A. Croyle, RPh, PhD, The University of Texas at Austin, College of Pharmacy, PHR 4.214D, 2409 University Avenue, Austin, TX 78712-1074, USA.

E-mail: macroyle@austin.utexas.edu



Table 1. Stability of marketed RNA LNP-based products

	Comirnaty	Spikevax	Onpattro
Vector	mRNA LNPs	mRNA LNPs	siRNA LNPs
Indication	vaccine against SARS-CoV-2	vaccine against SARS-CoV-2	polyneuropathy of hereditary ATTR amyloidosis
Manufacturer	Pfizer BioNTech	Moderna	Spark Therapeutics
Storage	−80°C long term 4°C 10 weeks 25°C 12 h	−50°C to −15°C long term 4°C 30 days 25°C 24 h	4°C 3 years 25°C 14 days
Formulation	for each 0.3-mL dose, 0.01 mg potassium chloride, 0.01 mg monobasic potassium phosphate, 0.36 mg sodium chloride, 0.07 mg dibasic sodium phosphate dihydrate, and 6 mg sucrose	for each 0.5 mL dose, 0.31 mg tromethamine, 1.18 mg tromethamine hydrochloride, 0.043 mg acetic acid, 0.20 mg sodium acetate trihydrate, and 43.5 mg sucrose	disodium hydrogen phosphate heptahydrate, potassium dihydrogen phosphate anhydrous, sodium chloride

impurities associated with lipid components.¹⁵ Each of the currently marketed COVID-19 vaccines are formulated as frozen buffered solutions containing sucrose (Table 1).^{16–18} While each of these products has been shown to be stable in solution at 4°C for up to 10 weeks, they must be discarded within 24 h at 25°C. In contrast, an LNP-based product containing short interfering RNA (siRNA) (Onpattro) is formulated as a buffered solution that is stable at 4°C for 3 years. This improved stability profile may be due to the short double-stranded structure of siRNA while mRNA and self-replicating RNA molecules are long single strands.

To date, there is limited information available regarding the stability of mRNA LNPs in the solid state. LNPs prepared in formulations containing more than 5% (w/v) of sugar demonstrated an increase in particle size prior to freeze-drying. This increased further once the lyophilization process was complete. Storage at 4°C or −20°C was required to conserve the physicochemical properties of the particles.¹⁹ Several reports were conflicting as transfection efficiency or *in vivo* bioactivity of lyophilized LNPs was not compromised even though notable drops in encapsulation efficiency and increases in particle size were detected once drying was complete.^{19,20} Taken together, this suggests that lyophilization cannot yet support storage of mRNA LNPs outside of the cold chain and that the physicochemical properties of an mRNA LNP-based product may not fully predict *in vitro* or *in vivo* performance.

The objective of the experiments summarized here was to evaluate a stabilization process that avoids cold denaturation and dramatic temperature fluctuations that occur during the freeze-drying process²¹ for its ability to stabilize mRNA LNPs under ambient conditions within a film matrix. This process has been shown to allow bacteria, enzymes, live adenovirus, adeno-associated virus (AAV), and plasmid DNA to be stored and shipped without refrigeration.^{22–24} A secondary objective was to understand how data collected from commonly accepted stability-indicating assays for LNP products can be used to predict bioactivity. Successful identification of a film-based formulation

that eliminates the need for ultra-low cold-chain storage and transport and identifying predictors of LNP performance will significantly improve access to these lifesaving medications and readiness for the next pandemic.

RESULTS

Stability of DNA complexes within the film matrix

We successfully preserved the transfection efficiency of naked plasmid DNA within an optimized film matrix after storage for up to 9 months at 25°C.²⁴ However, polyethyleneimine (PEI), a common transfection reagent that condenses DNA into positively charged complexes,²⁵ still had to be added to solutions prepared from rehydrated film for efficient cell entry. Thus, to simplify the transfection process for use in large-scale production of recombinant proteins and virus, we decided to evaluate the stability of pre-formed DNA complexes using either PEI or lipofectamine (LPF), a common lipid-based transfection reagent,²⁶ within the film matrix.

Plasmid:PEI complexes made in PBS supported comparable transfection efficiencies to those prepared in standard medium (Opti-MEM) during our screening process ($p > 0.18$, Figures 1A and 1B). Plasmid:PEI complexes stabilized in films prepared with gelatin were able to maintain full transfection efficiency (103.2%–111.6%) with respect to freshly made complexes in medium. Complexes prepared in medium and left at room temperature (RT) during the drying process retained only 12.2%–14.1% of the original transfection capacity (RT control, Figure 1A). Complexes in films prepared with gelatin were able to maintain a high level of transfection efficiency after 7 days (pH 5, 83.2% ± 1.2%; pH 8, 93.4% ± 4.5%) and 14 days (pH 5, 73.3% ± 1.9%; pH 8, 71.1% ± 7.1%) at 25°C (Figure 1B). The pH of the film matrix significantly affected the stability of PEI-DNA complexes prepared in Opti-MEM after 14 days at 25°C (pH 5, 64.9% ± 3.6% and pH 8, 34.1% ± 3.0% respectively).

Formation of DNA-lipofectamine (LPF) complexes was optimized by altering the volume of medium utilized to dilute plasmid and

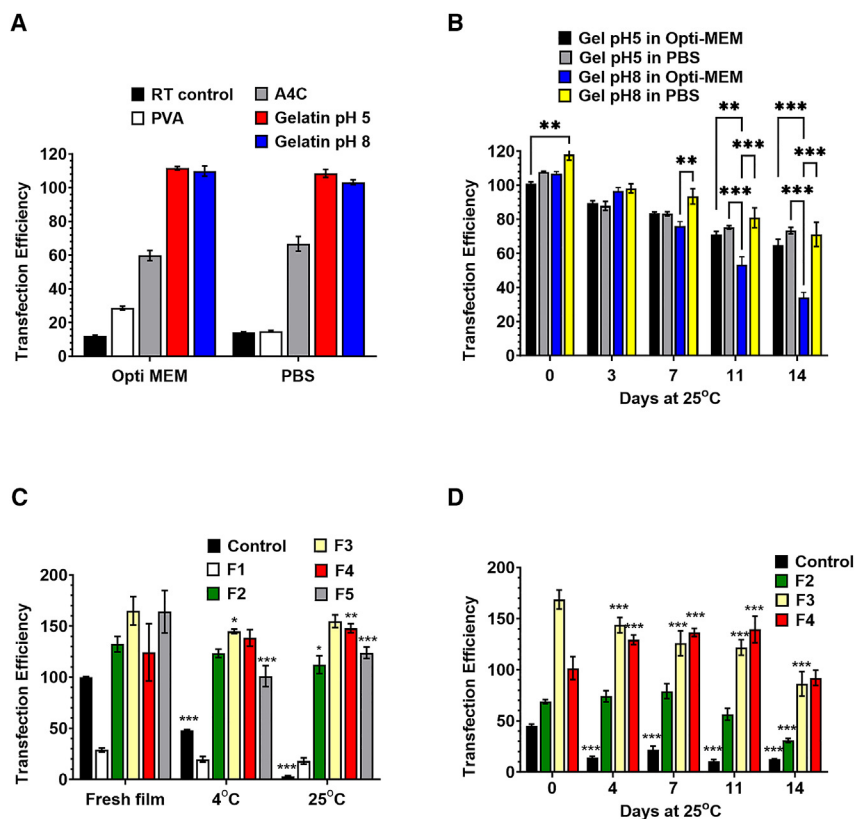


Figure 1. Transfection efficiency of DNA complexes is maintained within a film matrix

(A) Impact of medium used to form DNA:PEI complexes and polymer on preservation of transfection efficiency during the film-forming process. (B) Stability of PEI-DNA complexes in films stored at 25°C, 60% RH for 2 weeks. (C) Stability of LPF-DNA complexes within films after 4 days at 4°C and 25°C. (D) Stability of LPF-DNA complexes over 14 days at 25°C. (C and D) Control: LPF-DNA complexes stored in liquid medium alone. Information about specific formulations is summarized in Table S1. In each panel, data represent the average \pm the standard error of the mean of four replicates for each formulation. Statistical significance between formulations with respect to unformulated complexes stored under the same condition was determined by two-way ANOVA followed Tukey's (B) or Dunnett's (C and D in comparison to day 0 films) multiple comparison tests. * $p < 0.05$, ** $p < 0.01$, *** $p < 0.001$.

lipofectamine individually prior to mixing (Figure S2A). The highest levels of transfection were achieved by placing 1 μ g of DNA in 10–12.5 μ L of medium. This was 15-fold higher than what is recommended by the manufacturer (1 μ g DNA in 50 μ L of medium). Lipoplexes in films prepared using gelatin (pH 5, P3 and pH 8, P4) and different types of hydroxypropyl methyl cellulose (HPMC) (P6 and P7) retained more than 80% of the original transfection efficiency during the film-forming process, while those in films made with chitosan (P1), pectin (P2), and alginate (P8) did not support transfection at all (Figure S2B). Formulations F2, F3, and F4 (Table S1) preserved the transfection efficiency of LPF-DNA complexes within the film matrix after 4 days at either 4°C or 25°C, while transfection efficiency of complexes in medium alone (control) fell to 48.0% \pm 0.3% at 4°C and 3.2% \pm 0.2% at 25°C (Figure 1C). Formulations F3 and F4 retained 86.2% \pm 6.0% and 92.0% \pm 3.7% of their original transfection efficiency after 14 days at 25°C, while complexes in medium alone fell to 12.6% \pm 0.1% (Figure 1D). Taken together, we have demonstrated that embedding DNA complexes within the film matrix was necessary to preserve transfection efficiency during storage at 25°C as complexes stored in buffer under the same conditions precipitated and failed to transfect cells after 24 h at the same condition. It was also clear that LPF-DNA complexes were more stable than those formed with PEI, as transfection efficiency never fell below 90% during the 14-day period. Thus, we decided to evaluate the stability of mRNA LNPs within a film matrix.

mRNA LNP formulation development: pH and polymer base

Since gelatin-based films prepared in buffers of pH 5 and pH 8 preserved transfection efficiency of DNA complexes within the film matrix, the impact of pH on mRNA-containing LNPs was evaluated (Figure 2). The average particle size and polydispersity index (PDI) of the LNPs in liquid formulations buffered at pH 6 and pH 6.5 increased after 3 days at 4°C (Figure 2A). Encapsulation efficiency was also reduced; however, transfection efficiency remained high under these conditions (Figure 2B). The average particle size and PDI of LNPs significantly increased in formulations prepared with K100LV HPMC at pH 7–9 during the film-forming process ($p = 0.007$, Figure 2C). However, LNPs in formulations buffered at pH 8 and 9 had a transfection efficiency of 83.2% \pm 10.6% and 165.8% \pm 14.0%, respectively, despite a drop in encapsulation efficiency (Figure 2D). Therefore, Tris buffer, pH 8, was chosen for use in additional formulation screening studies.

Gelatin-based formulations that preserved transfection efficiency of DNA complexes did not support stability of LNPs (Figures 3A and 3B). LNPs placed in this formulation (P8) experienced a notable increase in particle size from 136 to 222 nm and associated polydispersity index (PDI) from 0.055 to 0.338 (blue dots, Figure 3A). Transfection efficiency also fell to 30.7% \pm 7.8%. Screening of additional polymers revealed that formulations containing different types of hydroxypropyl methyl cellulose (P1–P3) could maintain transfection efficiency with moderate increases in particle size and PDI during the film-forming process. Formulations containing hydroxyethyl cellulose (P4), Wallocel (P5), pullulan (P6), and poly vinyl acetate (PVA) (P7) formed large aggregates (Figure 3A) that could not enter cells to express the luciferase transgene (Figure 3B). LNPs formulated with K100LV had properties (particle size, 189 nm; PDI, 0.297; transfection efficiency, 96.7%) very similar to those of the original stock solution (Figure S3).

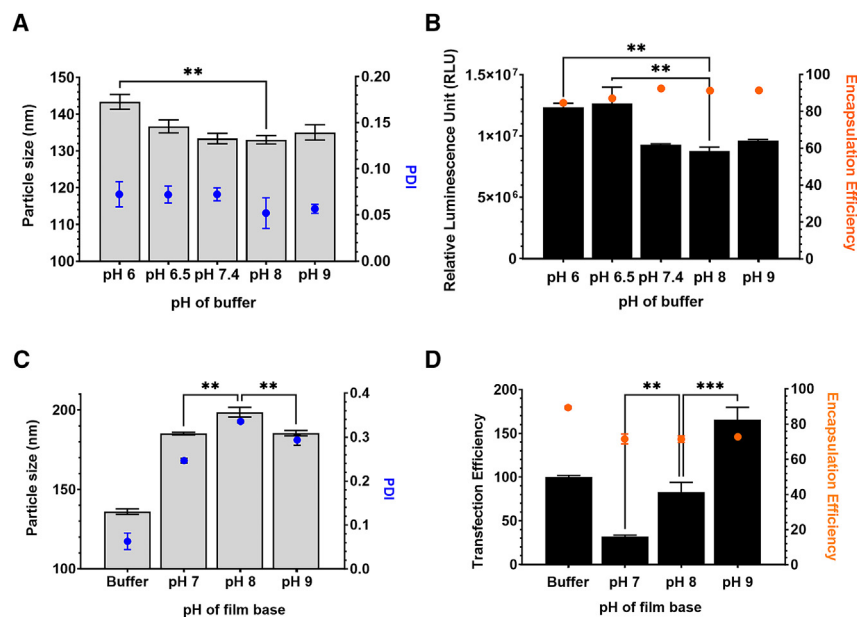


Figure 2. Impact of pH on LNP stability in solution and within the film matrix

Particle size (gray bars, A), polydispersity index (PDI, blue dots, A) and encapsulation efficiency (orange dots, B) demonstrate modest changes with respect to solution pH, while transfection efficiency (black bars, B) was significantly lower when LNPs were stored in solutions of pH 7.4–9 for 3 days at 4°C. mRNA LNP-containing films prepared with K100LV HPMC were more sensitive to formulation pH as significant changes in particle size and PDI (blue dots, C) and transfection and encapsulation efficiency (orange dots, D) were observed with respect to an unthawed stock solution (buffer) as pH increased. In each panel, data represent the average \pm the standard error of the mean for three replicates for each formulation. Statistical analysis was conducted with two-way ANOVA and Dunnett's *post hoc* test in which properties of LNPs in a formulation were compared to those seen in the original stock preparation. ** $p < 0.01$, *** $p < 0.001$.

mRNA LNP formulation development: Glycerol and surfactants

Glycerol (2.5% v/v) was initially used as a plasticizer in all of our film formulations to date.^{23,27} Increasing glycerol from 2% to 4% significantly reduced particle size from 199 to 161 nm and PDI from 0.336 to 0.131 ($p < 0.001$, Figure 3C) with no significant change in transfection efficiency (2% glycerol, $83.2\% \pm 10.6\%$ vs. 4% glycerol, $71.8\% \pm 5.9\%$, $p = 0.63$ Figure 3D). Films made with 8% glycerol were soft like hydrogels and took significantly longer to fully form a solid film. Addition of the hydrophilic, non-ionic surfactant, Pluronic F127, to the film matrix produced smaller, more homogeneous LNPs upon rehydration (base, Figure 3E). This also significantly improved transfection efficiency ($189.1\% \pm 9.7\%$, Figure 3F). This effect was more pronounced when Pluronic F127 was mixed with the LNP stock prior to mixing with bulk film formulation (LNP, particle size, 159 nm; PDI, 0.137; EE, 83.0%; transfection efficiency, 234.4%). While these results seemed promising, formulations prepared by adding the surfactant to the LNP stock prior to addition to the bulk formulation significantly increased particle size (152 ± 6 nm to 213 ± 7 nm) and PDI (0.122 ± 0.027 to 0.354 ± 0.018) after storage within a film matrix at 4°C for a week with a corresponding drop in transfection efficiency ($127.5\% \pm 5.4\%$ to $33.5\% \pm 5.2\%$, no PEG lipid, Figure 4).

mRNA LNP formulation development: PEG lipids

Two PEG lipids commonly utilized for fabrication of LNPs, N-(methylpolyoxyethylene oxycarbonyl)-1,2-dimyristoyl-sn-glycero-3-phosphoethanolamine sodium salt (DMPE-PEG) and 1,2-dimyristoyl-rac-glycero-3-methoxypolyethylene glycol-2000 (DMG-PEG), were included as excipients in the film matrix at two concentrations: 0.008% (low) and 0.04% (high). Inclusion of these excipients in the film base did significantly improve particle size and PDI with respect to formulations that did not contain extraneous lipid (no PEG lipid, 152 ± 6 nm vs. low DMPE-PEG, 143 ± 1 nm, $p = 0.61$; vs. high

DMPE-PEG, 131 ± 4 nm, $p = 0.01$; Figure 4A). The impact of the PEG lipid on stability within the film matrix was more defined after 7 days at 4°C as particle size increased in films without PEG lipid (213 ± 7 nm) while that in low-DMPE-PEG and high-DMPE-PEG formulations remained at 166 ± 1 nm and 126 ± 5 nm, respectively ($p < 0.001$). Despite improvements in particle size, high concentrations of extraneous lipid made LNPs “leaky” with encapsulation efficiencies of $36.2\% \pm 3.3\%$ (DMPE-PEG) and $56.2\% \pm 0.4\%$ (DMG-PEG; Figure 4C). Transfection efficiency followed a similar trend in freshly prepared films ($10.3\% \pm 1.7\%$) (DMPE-PEG) and $37.9\% \pm 11.3\%$ (DMG-PEG, Figure 4D). Low concentrations of extraneous PEG lipid did not compromise encapsulation and transfection efficiencies during the film-forming process (day 0, red and dark blue bars, Figures 4C and 4D). Despite these findings, transfection efficiency of LNPs in these preparations fell to $76.5\% \pm 10.6\%$ (DMPE-PEG) and $66.9\% \pm 13.2\%$ (DMG-PEG) after 7 days at 4°C, prompting further revision of the film formulation.

mRNA LNP formulation development: Polymer viscosity

Initial screening of film-forming polymers was conducted with low-viscosity preparations for ease of dissolution and for potential use as injectable products (Figures 3A and 3B). Since the optimal polymer from those studies (K100LV HPMC) could not support long-term stability of mRNA-containing LNPs, we decided to evaluate stability in a high-viscosity polymer shown to be superior to the low-viscosity polymer used in our studies for stabilization of AAV9 within a film matrix (K4M HPMC).²³ Mixing the polymers (K4M and K100LV HPMC) at different ratios generated solutions with viscosities ranging from 56 to 169 cps (Table S2). LNPs in films prepared with these formulations had comparable particle size (162–193 nm), PDI (0.158–0.261), and encapsulation efficiency (80.0%–87.5%) values (Figures S4A–S4C). Transfection efficiency was 2- to 4-fold higher than that seen from an LNP stock

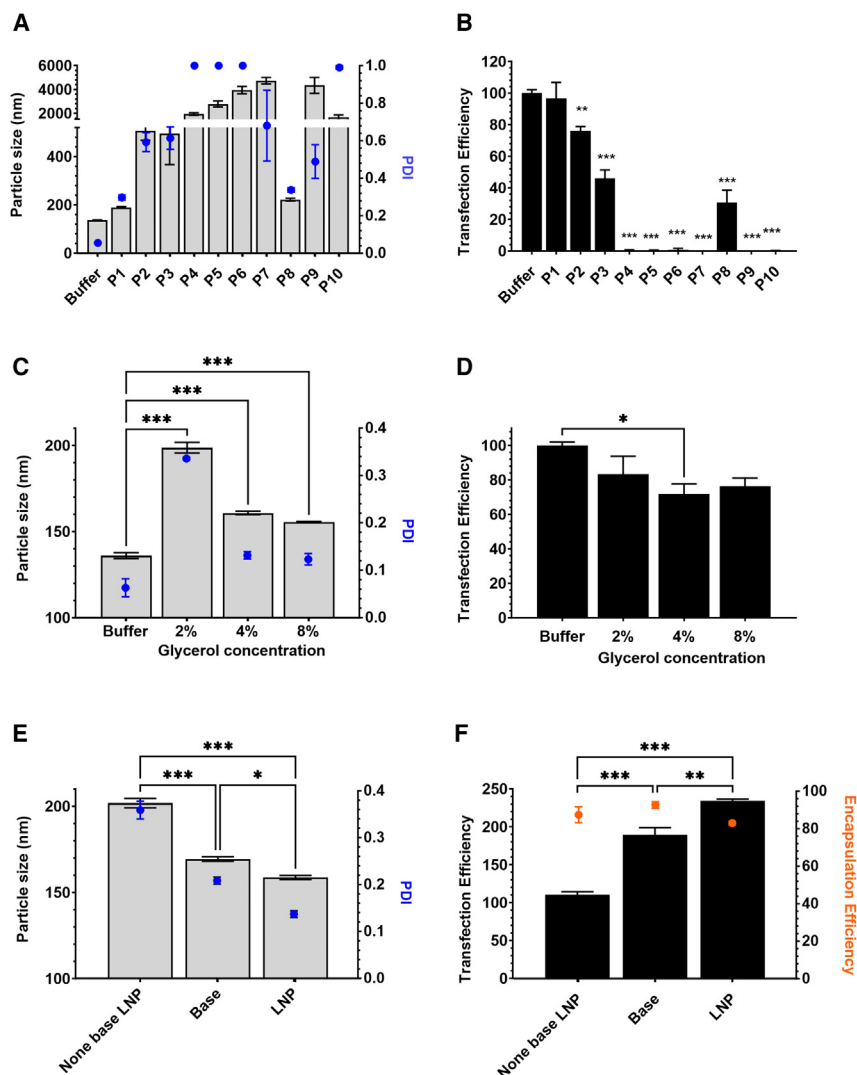


Figure 3. Impact of excipients on the preservation of physical and biological properties of LNPs during the film-forming process

(A and B) LNPs were placed in low-viscosity polymer formulations and films formed under constant airflow under ambient and aseptic conditions. Films were then reconstituted for analysis and LNPs compared to a frozen stock solution (buffer). (C) Glycerol improves integrity of mRNA LNPs within the film matrix. Concentrations above 2% v/v maintain particle size and PDI (blue dots) of LNPs with respect to an unfrozen stock solution (buffer). (D) Impact of glycerol on transfection efficiency of LNPs during the film-forming process. (E) Addition of Pluronic F127 to LNPs before incorporation into the film matrix significantly reduces particle size and PDI (blue dots) during the film-forming process. Pluronic F127 was added either directly to the film formulation (1.5% K100LV, 3% glycerol) before mixing with LNPs (base) or to the LNP stock prior to mixing with the bulk formulation (LNP). (F) Impact of mixing Pluronic F127 with LNP stock prior to mixing with the film matrix on encapsulation (orange dots) and transfection efficiency. Specific details of formulations are summarized in Table S1. In each panel, data represent the average \pm the standard error of the mean for three replicates for each formulation. Statistical significance with respect to freshly thawed LNPs in Tris buffer was determined by two-way ANOVA and Dunnett's *post hoc* tests. * $p < 0.05$, ** $p < 0.01$, *** $p < 0.001$.

solution stored frozen (Figure S4D, buffer). After 4 weeks at 4°C, a significant increase in particle size and drop in transfection efficiency was found in all formulations tested. Since formulations containing only the low- (F20) or high-viscosity (F24) polymers showed the least change in particle size (268 ± 43 and 234 ± 14 , respectively) and the best encapsulation efficiencies ($82.6\% \pm 1.2\%$ and $80.8\% \pm 2.3\%$, respectively), additional studies with films containing each polymer and several different phospholipids were conducted (Figure S4).

LNPs in films prepared with K4M and PEG lipids demonstrated a significant increase in particle size (DMPE-PEG, 168–193 nm; DMG-PEG, 163–215 nm; Figure S5A) as well as a significant decrease in encapsulation efficiency (DMPE-PEG, 80%–63%; DMG-PEG 80%–59%, Figure S5C) after 28 days at 4°C. Films containing K4M and the phospholipid 1,2-dimyristoyl-sn-glycero-3-phosphocholine (DMPC) supported minimal changes in particle size (150–160 nm) and PDI (0.195–0.215; Figures S5A and S5B) and encapsulation effi-

ciency (85%–79%) after 28 days at 4°C. Despite this, transfection efficiency of LNPs in this formulation was very low after the film-forming process was complete ($47.0\% \pm 4.5\%$, D0) and 28 days at 4°C ($14.4\% \pm 3.8\%$; Figure S5D). Degradation of LNPs in formulations prepared with the low-viscosity polymer occurred at a much faster rate. Significant increases in particle size were found in these preparations after 14 and 28 days at 4°C (on day 14, DMPE-PEG 171 ± 9 nm, DMG-PEG 270 ± 26 nm, DMPC 275 ± 6 nm; and on day 28, DMPE-PEG 309 ± 17 nm, DMG-PEG 348 ± 37 nm, DMPC 288 ± 19 nm; $p < 0.001$; Figure S5A). A similar trend was seen with respect to encapsulation efficiency (day 14, DMPE-PEG $67.7\% \pm 4.6\%$, DMG-PEG $44.8\% \pm 9.1\%$, DMPC $46.7\% \pm 4.0\%$; and day 28, DMPE-PEG $48.7\% \pm 6.2\%$, DMG-PEG $26.4\% \pm 4.9\%$, DMPC $47.2\% \pm 1.0\%$; Figure S5C). However, transfection efficiencies of LNPs in these preparations were similar to those in formulations containing the K4M polymer (Figure S5D).

mRNA LNP formulation development: Surfactant combinations

In order to improve LNP stability within the film matrix further, an additional study in which non-ionic surfactants, often used in pharmaceutical formulations to prevent aggregation and in suspension culture medium to protect cells from hydrodynamic and bubble-induced shear,^{28,29} were combined with Pluronic F127. Addition of a second surfactant did not significantly affect particle size,

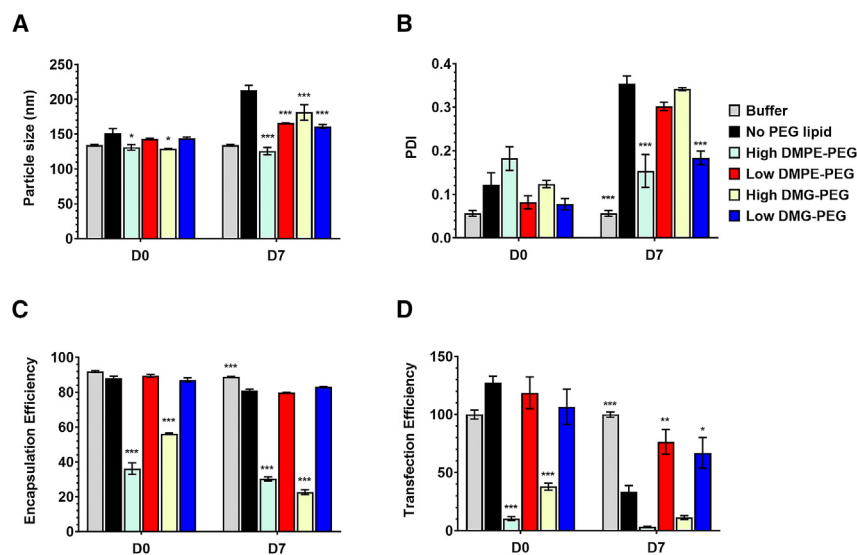


Figure 4. Use of PEG-conjugated lipids as excipients improves LNP stability within the film matrix at 4 °C

PEG-conjugated lipids were included in bulk film formulation (1.5% K100LV + 3% glycerol + 0.01% Pluronic F127) at high (0.04%) and low (0.008%) concentrations. Freshly prepared films (D0) and those stored at 4°C for a week (D7) were re-hydrated for measurement of particle size (A), PDI(B), encapsulation (C), and transfection (D) efficiency. Data generated from frozen stock LNPs stored at 400 µg/mL (buffer) are included for comparison. In each panel, data represent the average ± the standard error of the mean for three replicates for each formulation. Statistical analysis between formulations with and without PEG lipids was determined using two-way ANOVA and Dunnett's *post hoc* tests. **p* < 0.05, ***p* < 0.01, ****p* < 0.001.

increased to 197% ± 19.2% after 2 weeks at 4°C. Since our goal was to preserve the LNP properties of the original stock formulation, a buffer of pH 8.5 was chosen for use further formulation refinement studies.

mRNA LNP formulation development: Amino acids and EDTA in an optimized formulation

In a final attempt to further improve the thermostability of mRNA-containing LNPs, compounds found to stabilize plasmid DNA within the film matrix for up to 9 months at RT²⁴ were added to the optimized formulation (OF). Arginine, a cationic, alkaline amino acid, significantly enhanced transfection efficiency of LNPs stored within the film matrix after 2 (241.5% ± 9.5%), 4 (268.5% ± 10.7%), and 16 weeks (175.7% ± 44.6%) (Figure 6D). A similar effect was seen when EDTA, a chelating agent, was added to the OF. This preparation supported LNPs with transfection efficiencies consistently above 200% for 16 weeks at 4°C. Each of these formulations was also able to maintain particle size, PDI, and encapsulation efficiency of LNPs throughout the 16 week study period (Figures 6A–6C). It is also important to note that the OF alone was also capable of maintaining bioactivity throughout the first 4 weeks at 4°C (89.8%–103.4%) and dropped below 18% soon after that. The incorporation of cysteine, known to prevent oxidation, did not significantly improve transfection efficiency at the 2 week time point (103% ± 7.7%) but did improve this value at 4 weeks (210.3% ± 14.3%; Figure 6D). Since this formulation did not perform as well as the original OF with arginine or EDTA, it was not followed beyond the 4-week time point.

Manufacturing and storage conditions

Films were prepared with the OF formulation (Table S1) under constant airflow at 20°C in chambers set at 52.5%, 49%, 45%, and 40% relative humidity (RH). For each condition, films were collected when they appeared dry by visual inspection (sufficient drying) and an hour later (extended drying; Figures 7A and 7B). The time in which film forming was complete was significantly reduced in low-humidity environments. LNPs in films prepared under the sufficient-drying protocol were of similar particle size (Figure 7A). PDI increased as RH decreased

PDI, and transfection efficiency of LNPs during the film-forming process (D0; Figure S6). However, encapsulation efficiency was significantly reduced by all formulations tested except the formulation containing Pluronic F68 and F127 (D0; Figure S6C). After 2 weeks at 4°C, LNPs in formulations containing surfactant combinations had significantly better physical characteristics than those prepared with Pluronic F127 alone. Formulations containing Pluronic F68 and Brij 58 had the lowest particle size (151 ± 1 nm and 155 ± 4 nm) and PDI (0.150 ± 0.001 and 0.184 ± 0.001) of all formulations tested (Figures S6A and S6B). While encapsulation efficiency was significantly reduced in all formulations tested at the day 14 time point, the formulation containing Pluronic F68 maintained the highest value (77.4% ± 0.5%). Despite these results, transfection efficiency was reduced by approximately 40% in all formulations tested (D14; Figure S6D).

mRNA LNP formulation development: pH of film base

We have previously found that changes in pH within the film matrix during the film-forming process can significantly affect stability of recombinant viruses.^{22,23} Screening of several different film formulations revealed that the pH of films prepared with 10 mM Tris pH 8 dropped to 6.5 and that sucrose (10%) in the same buffer reduced pH further to 6.0, while those prepared with PBS fell to 5.5 (Table S3). Internal film pH did not affect the physical and biological characteristics of LNPs during the film-forming process (D0; Figure 5). After 14 days at 4°C, the particle size and PDI of LNPs in formulations prepared with pH 7.4 buffer increased to 242 ± 17 nm and 0.365 ± 0.030, respectively (Figures 5A and 5B). Despite this, encapsulation efficiency remained high (82% ± 0.6%) and transfection efficiency was 62.8% ± 3.4% (Figures 5C and 5D). LNPs stored in films prepared with buffer at pH 8.5 maintained optimal particle size (149 ± 1 nm), PDI (0.139 ± 0.009), encapsulation (82.6% ± 0.9%), and transfection (103.9% ± 6.3%) efficiencies. While those prepared with buffer at pH 9 had similar properties, transfection efficiency

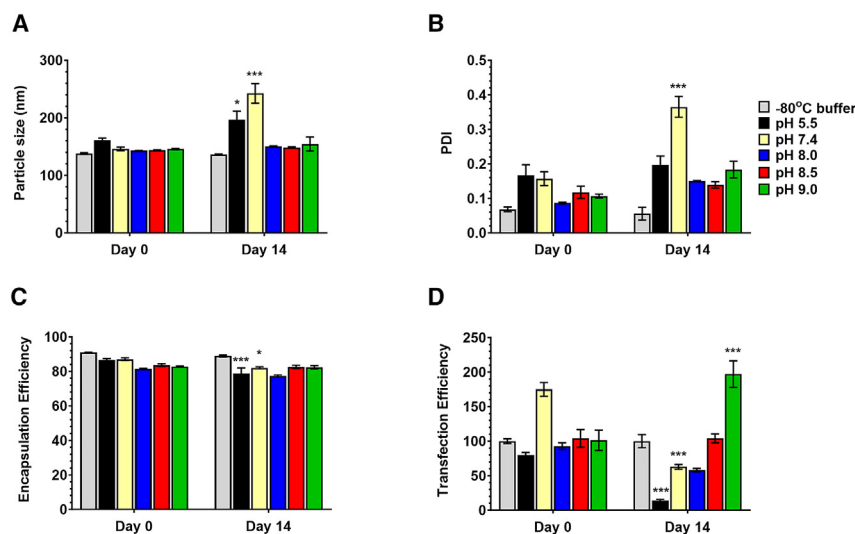


Figure 5. Buffers of pH 8.5 preserve physical and biological properties of LNPs within the film matrix during storage at 4°C

Film base was prepared with several different buffers ranging in pH from pH 5.5 to 9.0. The internal pH of films prepared with these buffers and their composition is summarized in Table S3. Films were rehydrated with 10 mM Tris buffer pH 8 to determine particle size (A), PDI(B), encapsulation efficiency (C), and transfection efficiency (D). In each panel, data represent the average \pm the standard error of the mean for three replicates for each formulation. Statistical significance between measurements taken on day 0 and day 14 within the same formulation was determined by two-way ANOVA and Sidak's multiple comparison tests. * $p < 0.05$, *** $p < 0.001$.

(blue dots, Figure 7A). Extending the drying time by 1 h significantly increased LNP particle size (from 160 to 262 nm in the order of decreasing humidity) and PDI (from 0.293 to 0.462) while encapsulation (from 73.5% to 45.5%) and transfection (from 128.6% to 75.2%) efficiencies were significantly reduced (Figure 7B).

LNPs stored within the film matrix at 25°C for 14 days demonstrated a slight increase in particle size (193 ± 29 nm) and PDI (0.199 ± 0.042), while encapsulation efficiency remained at $81.6\% \pm 1.7\%$ and transfection efficiency fell to $2.7\% \pm 0.6\%$ (Figures 7C and 7D). LNPs in films stored at -20°C did not experience a significant change in physical and biological properties over the 14-day period. The impact of environmental humidity on LNP stability within the film matrix was studied at 4°C. RH did not significantly affect particle size, PDI, or encapsulation efficiency of LNPs stored within the film matrix (Figures 7E and 7F). Transfection efficiency was compromised after 14 days at 4°C regardless of the RH of the storage chamber ($102.9\% \pm 11.4\%$, fresh film vs. 24.3%–40.0% in the order of decreasing humidity; Figure 7F). Taken together, these data suggest that storage temperature, not RH, significantly affects the transfection efficiency of mRNA LNPs stored within the film matrix.

DISCUSSION

In this report, we evaluate the impact of a variety of parameters associated with incorporation of mRNA LNPs within a film matrix using current, gold-standard metrics for LNP performance. Particle size, PDI (a measure of the heterogeneity of the particle size), and encapsulation efficiency provide information about the physical characteristics of LNPs and provide insight into the structure and integrity of the particles. Transfection efficiency is utilized to assess *in vitro* activity and to possibly predict *in vivo* performance, which requires the mRNA and lipid particle to be intact. Data summarized here demonstrate that results obtained from these assays can be conflicting. Particle size, PDI, and encapsulation efficiency generally follow the same trend. An increase in particle size and PDI suggests that the lipid

layers of the particle within a formulation are compromised. Particles that may be compromised during the film-forming process or during long-term storage release mRNA originally contained within the particle. This is measured as a reduction in encapsulation efficiency with respect to the original stock LNPs. However, one must realize that the current assay utilized to measure encapsulation efficiency relies upon the binding of RNA to a fluorescent dye and the readout interpreted as the amount of RNA released from the particle. A change in RNA content (due to degradation) or RNA structure due to loss of interaction with carrier lipids (needed for mRNA to effectively enter and escape the endosome) significantly affects transfection efficiency but may not fully be detected by assays currently used to describe the physical properties of LNPs.³⁰ When assessing transfection efficiency of mRNA LNPs broadly across the literature, one must also critically evaluate factors that vary considerably between different research groups and significantly affect results obtained from this assay, such as cell line and method for normalization of data (i.e., by cell number or protein content).

The biggest hurdle to stabilization of mRNA-containing lipid nanoparticles in liquid formulations is keeping the lipid network of the particle in the lowest energy state. As lipid molecules flex, the energy associated with this molecular motion rises, slowly increasing particle size in a manner that supports aggregation, fusion, or eventual disruption of the particle.³¹ Molecular flex can also facilitate particle degradation initiated by electrophilic impurities present in ionizable stock chemicals utilized to prepare LNPs and/or formulate LNP-based products and that collect during long-term storage in formulated products. These impurities can accelerate RNA degradation within the particle, often at a pace faster than free RNA in solution.^{15,32} This process accelerates as temperature rises and molecular motion increases or when stabilizing water molecules are removed from around the lipid shell during the film-forming process (Figure S1). During this process, the RNA can shift to the aqueous phase of the particle, which accelerates degradation through hydrolysis and oxidation. This shift can also occur during freezing; however, molecular motion is then suspended in the frozen and/or solid state. When films

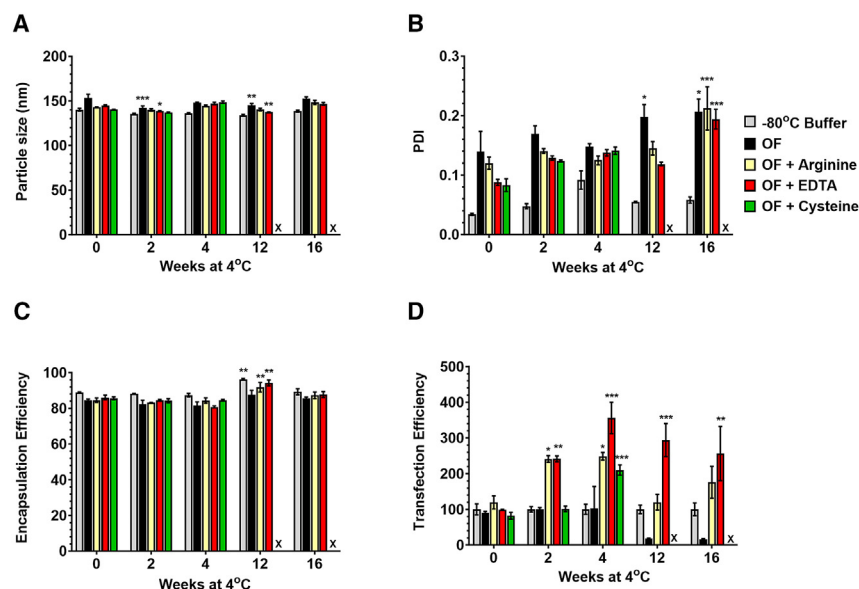


Figure 6. Excipients that prevent degradation of recombinant DNA within a film matrix significantly improve LNP stability at 4°C for 16 weeks

Arginine (0.05%), cysteine (0.005%), and EDTA (1 mM) were added individually to an optimized formulation (OF) (Table S1). Films were stored at 4°C for 16 weeks and rehydrated with 10 mM Tris buffer pH 8 for measurement of particle size (A), PDI (B), encapsulation (C), and transfection efficiency (D). In each panel, data represent the average \pm the standard error of the mean for three replicates for each formulation. Statistical significance between LNP properties in aged films and fresh films (week 0) prepared with the same film formulation was determined by two-way ANOVA and Dunnett's multiple comparison tests. * $p < 0.05$, ** $p < 0.01$, *** $p < 0.001$.

prepared with the OF (at pH 8) were placed at -20°C , physical and biological parameters remained stable for at least 5 weeks (Figure S7); however, transfection efficiency was significantly compromised after 2 weeks at 4°C (Figure 7F). Kim et al. also found that *in vivo* activity of LNPs containing self-replicating RNA was reduced 2- to 4-fold after storage at 4°C for 7 days despite a superior stability profile at -20°C .¹⁴ Taken together, this highlights the challenge of stabilizing LNPs at temperatures above freezing and the complex roles excipients must fill to maintain LNP stability in the liquid and solid state.

Of the polymers assessed in these studies, hydroxypropyl methyl cellulose (HMPC) was the only polymer that did not compromise transfection efficiency during the film-forming process (Figure 3). HPMC is available in a variety of grades with different physical and thermal properties with respect to water absorption and water vapor and gas permeabilities.³³ It can also vary in molecular weight and hydroxypropyl/methoxy substituents that influence release of materials from films, their hydration capacity, and emulsion-stabilizing effects.^{34–37} Of the different grades tested, grade K was able to maintain the best particle shape and transfection efficiency (Figures 3A and 3B). This grade of HPMC contains the lowest methoxy content (19.0%–24.0%) with a hydroxypropyl content similar to that of the grade E material (7%–12%), suggesting that an optimal hydroxypropyl/methoxy substitution ratio is critical to form a protective matrix around the hydrophilic shells of the LNPs during the film-forming process and upon rehydration (Figures S4 and S5).

Because most mRNA LNP preparations are currently formulated as injectable products,^{2,3} initial formulation development focused on polymers with viscosities ranging from 56 to 169 cps (Figure S4; Table S2). Since the lowest-viscosity polymer (K100LV) performed poorly alone (Figure 4), it was mixed in various ratios with the high-viscosity polymer (K4M) in an effort to improve stability of the LNPs during the film-forming process. While all formulations tested

improved transfection efficiency of LNPs in freshly prepared films, those containing each polymer alone (K100LV in F20 and K4M in F24) showed an increase in particle size and a drop in encapsulation and transfection efficiency during storage at 4°C (Figure S4). An additional study was initiated to evaluate stability of LNPs in films prepared with the K100LV and K4M polymers individually. In these preparations, a PEG-conjugated lipid, a common component of the LNP, was added to the film matrix to support particle integrity during the film-forming process and long-term storage (Figure S5). Extraneous PEG-conjugated lipids added to LNP preparations at concentrations that far exceed the amount normally included within the particle structure (25%–60% vs. $\leq 15\%$ lipid molar content) have been utilized to maintain particle size during nebulization and improve delivery to the lung.⁹ While those concentrations cannot be supported in a film-based dosage form or an injectable product, we did find that a very small amount of the lipid (0.008%) maintained LNP stability while a higher concentration (0.04%) disrupted the particles during the film-forming process (Figure 4). DMPC, a PEG-free lipid, was also evaluated as an external excipient. While it could maintain the physical properties of LNPs, transfection efficiency was poor, suggesting that it formed a seal around the LNPs, making them too sturdy to release mRNA for transfection (Figure S5). It is important to note that the concentration of PEG-conjugated lipid used as an external excipient in our OF is significantly lower than 0.02%–0.035% w/w, the concentration of PEG lipid in marketed LNP particles.⁹ It does not inhibit cell entry and should not promote any toxic effects such as formation of anti-PEG antibodies as they were not detected in patients receiving multiple doses of LNP-based COVID-19 vaccines.² Interestingly, the high-viscosity polymer maintained the physical properties of the LNPs within the film matrix better than the low-viscosity polymer (Figure S5). This effect was also observed for an AAV9 vector that was successfully utilized as an injectable product.²³

Surfactants have been used to produce and stabilize solid lipid nanoparticles. They are generally added in the aqueous phase prior to mixing with the lipid phase containing the drug so that they are present

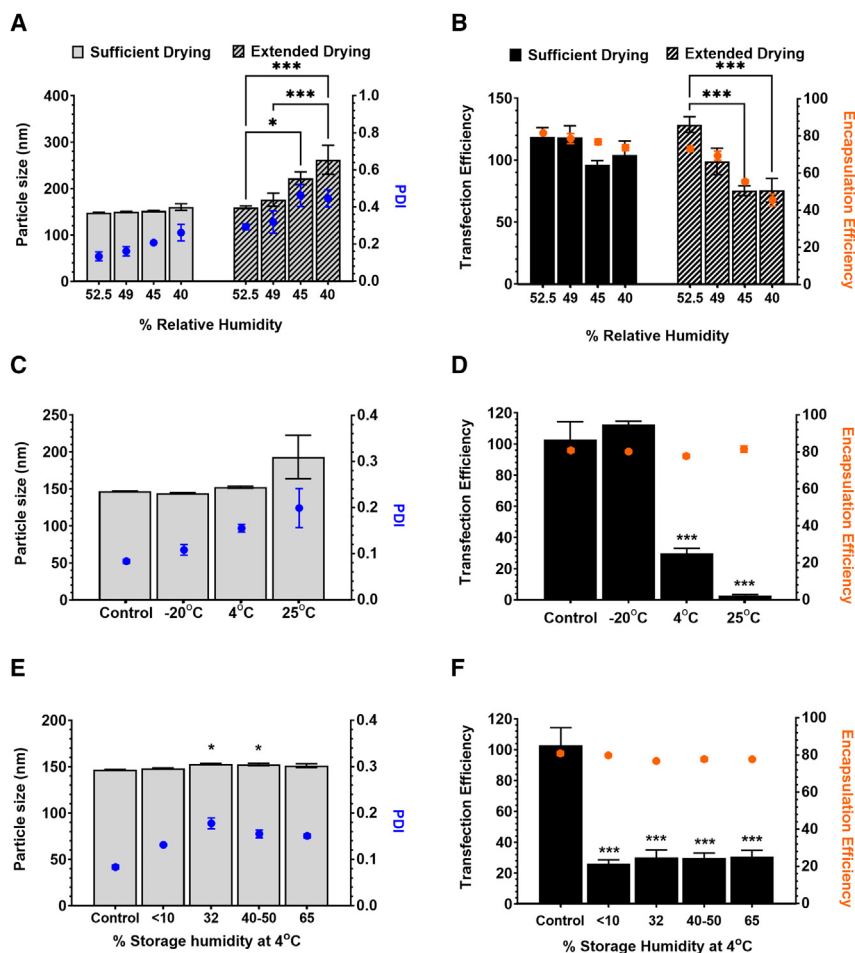


Figure 7. Manufacturing and storage conditions significantly affect physical and biological properties of mRNA LNPs within a film matrix

(A and B) LNPs were dried in a chamber under controlled airflow, temperature (20°C), and different RH environments. For each condition, four films were collected at two time points: sufficient drying, when films looked visually dry; and extended drying, 1 h after films were determined dry by visual inspection. Films were immediately rehydrated and analyzed for particle size and particle distribution (blue dots, A) and transfection and encapsulation efficiency (orange dots), (C and D) Impact of storage temperature on particle size (gray bars) and PDI (blue dots), encapsulation (orange dots), and transfection efficiency (black bars) of LNPs. (E and F) Impact of RH on particle size (gray bars) and PDI (blue dots), encapsulation (orange dots), and transfection efficiency (black bars) of LNPs. Different humidity conditions were established using desiccants or two-way humidity control packs. In each panel, films were prepared with OF (Table S1). In each panel, data represent the average \pm the standard error of the mean for three or four replicates for each condition. In (A) and (B), statistical differences between films prepared under each condition was determined by two-way ANOVA and Tukey's *post hoc* tests. In (C)–(F), statistical differences between freshly prepared and 2-week-old films stored under each of the described conditions were determined using two-way ANOVA and Dunnett's multiple comparison tests. * $p < 0.05$, ** $p < 0.01$, *** $p < 0.001$.

This suggests that the poly(ethylene oxide) (PEO)-poly(propylene oxide) (PPO)-PEO triblock copolymers when used at a concentrations much lower than their critical micelle concentra-

tions (Pluronic F127, 0.26–0.8 wt % Pluronic F68, 0.033–0.4 wt %) form a molecular dispersion of monomers as they are added to the viscous film base. Then, surfactant molecules form a network of protective micelles around the LNPs during the film-forming process as water is removed from hydrophilic groups.⁴³ Rehydration of the film matrix allows the Pluronic to be dispersed as monomers that align themselves with the PEG lipid and polymer base to maintain particle size and transfection efficiency of the LNP.

Glycerol is used to enhance the pliability and flexibility of film-based products. It is also an established cryoprotectant for cells, tissues, viruses, and liposomes through its ability to reduce ice crystal formation and changes in osmotic pressure during freezing.⁴⁵ It has been shown to maintain the lipid bilayer of liposomes during drying⁸ and can form hydrogen bonds with water and free hydroxide groups on LNPs. Because addition of sugars (i.e., sucrose, trehalose, isomalt) did not affect LNP properties in freshly prepared films or enhance 4°C stability, we believe that glycerol protects mRNA LNPs from dehydration and osmotic change during the film-forming process. It is important to note that the amount of glycerol needed to support LNP stability within the optimized film matrix was higher than that required to stabilize other biomolecules

on the particle surface.^{38,39} Surfactants are also a common component of film-based dosage forms as they facilitate spreading across the mold surface and wetting of the film during dissolution. They also lower the surface tension of the film matrix, which decreases water absorption properties of the HPMC base and makes hydrophilic groups less accessible to water molecules.³³ They have also been shown to play a key role in the thermostabilization and delivery of biological drugs.^{22,23,40} However, they were not considered in the early stages of this project since it was known that surfactants could easily disintegrate the LNP. Careful review of the literature revealed that a non-ionic surfactant, Pluronic F68, is an important component of chemically defined cell culture medium because it protects cells from hydrodynamic and bubble-induced shear in bioreactors²⁸ and has been used in commercial AAV gene therapy products to prevent aggregation.^{41,42} Adding it and Pluronic F127 to the LNP stock to a concentration of 0.006% prior to mixing with the polymer base did not alter the physical and biological properties of LNPs in fresh films and improved stability during storage at 4°C (Figure S6). This concentration was critical for maintaining LNP stability as lower concentrations (0.001%–0.003%) facilitated LNP aggregation after 14 days at 4°C (data not shown). Use of other amphipathic, non-ionic surfactants such as Tween 20, Tween 80, and Brij 58 were not as effective.

(Figure 3).^{22,23,40} This, paired with the fact that hydrogen bonding between plasticizers such as glycerol and polymers such as HPMC create pockets available for water molecules,³³ highlights the importance of packaging to prevent water absorption from the environment for film-based products.

Even though we identified a variety of excipients that collectively improved the physical properties of LNPs during drying and storage, transfection efficiency was still compromised. Transfection efficiency depends on both intact lipid shells and mRNA. Realizing that buffer pH can influence lipid and mRNA degradation, we found that low pH caused a rapid increase in particle size and loss of transfection in both liquid (pH 6–6.5; Figure 2) and dry formulations (pH 5.5–6.5; Figures 2 and 5) due to acid-mediated hydrolysis of lipids and mRNA. While it is known that strong bonds form between mRNA and ionizable lipids within the LNP, this could not prevent degradation during storage at 4°C (Figure 5). This also explains why mRNA-based COVID-19 vaccines are formulated at pH 7.5–8 (Table 1), although there are suggestions that keeping the pH below the pKa of the lipids is needed to maintain transfection and stability.⁴⁶ Increasing the internal pH of the film to ≥ 7 , or preparing the film base at pH 8.5–9.0, delayed degradation and significantly improved mRNA LNP stability for 2 weeks at 4°C (Figure 5).

In addition to formulation design, operation parameters play a notable role in stabilizing mRNA LNPs within a film matrix. An environment of 52.5% RH did not compromise LNP characteristics during a sufficient and extended drying cycle (Figure 7). Lower humidity and longer drying times damaged LNPs during the film-forming process, as shown by increased particle size and reduced encapsulation and transfection efficiencies. mRNA LNPs contain a significant amount of internal water (24% \pm 2%).¹⁰ Films prepared with our OF contain 22%–25% residual water after drying, suggesting that the drying process must maintain equilibrium between the environment within the LNP and that within the film matrix. Taken together, this suggests that manufacturing films in a low-RH environment, extending a drying cycle beyond the time that film formation is complete, and use of formulations with different tonicity disrupt this balance, causing the LNPs to collapse or swell in the final product. While environmental humidity was found to affect the long-term stability of adenovirus, AAV, and plasmids at 25°C and 40°C within a film matrix,^{22–24,40} it did not significantly affect LNP stability at 4°C (Figure 7). This effect will be studied over a longer duration and eventually at higher temperatures in our laboratory.

The clinical success of mRNA LNPs within the last 2 years has accelerated our understanding of the LNP-based delivery platforms and inspired a wave of innovation with respect to RNA structure, lipid compositions, and manufacturing processes that can affect the physical and biological properties of LNPs. Thus, it is not clear how our OF and development approach will translate to other mRNA LNP compositions. Rapid expansion of the field has also led to the realization that there are few regulated standards on mRNA LNP products. While transfection efficiency is one of the key parameters that progresses a product to clinical use, it can be variable with mRNA

LNP-based products. To address this issue, freshly thawed mRNA LNPs stored at -80°C were included in each transfection experiment as the standard by which to compare LNP stability in freshly prepared films and within the film matrix during long-term storage.

Stabilization of the intricate structure of mRNA LNPs required methods that restrict the molecular motion of the particles and their payloads. This was achieved by storage of a liquid formulation at ultra-low temperatures to quickly distribute a vaccine to mitigate a surging number of infections during the COVID-19 pandemic. However, it also posed a significant barrier to rapid and efficient distribution of vaccines to many countries around the globe, such as Vietnam, whose Expanded Program on Immunization had no capacity for storing vaccines at -80°C to -70°C .⁴⁷ Here, we have identified an optimized formulation containing a panel of hydrophilic excipients that created a preparation with a slightly increased particle size (<10 nm), a decrease of 5% in encapsulation efficiency, and no loss in transfection efficiency for 16 weeks (Figure 6). This, paired with the report that LNPs in the range of 60–150 nm retained immunogenicity in non-human primates, suggests that a modest increase in LNP particle size is not indicative of poor LNP clinical performance.³⁸ While 16 weeks may not seem like a significant period of time for the stability profile of a drug product, the first doses of Comirnaty reached clinical testing sites 41 days after manufacture, which is well within the stability profile of our formulation.⁴⁸ This, paired with the development of a global network of manufacturing sites, could significantly improve last-mile distribution and access to mRNA vaccines to communities that need them the most.

The results summarized here represent a notable transition in the search for stabilization technologies that remove the need for frozen storage for mRNA LNP-based products. The films utilized in these studies were prepared from excipient stock solutions that were sterile filtered. Films were dried, peeled, and packaged in particle-free bags under HEPA filtered airflow. We envision scaled-up production of films to involve dispensing formulations containing LNPs in unit dose molds similar to foil blister packs in which films are dried under class 100 conditions. Once drying is complete, molds are heat sealed. Transport of these blister packs would be space and resource sparing compared to traditional glass vials and syringes. While our data support stability of LNPs if films were inadvertently frozen, which sometimes happens during storage under refrigerated conditions⁴⁹ (Figure S7), it is not clear how repeated freeze-thaw cycles would affect LNP stability within our optimized film matrix. This may be of concern given that our films contain significantly more moisture than what was found for adenovirus- and AAV-containing films, which offered protection over a series of 16 freeze-thaw cycles.^{22,23} At the point of use, a syringe can be used to inject sterile saline into the mold to dissolve the film and the resulting solution drawn up for injection. To our knowledge, this is the first report in which criteria for stabilization of mRNA LNPs within a film matrix has been extensively characterized. Studies to build upon this work and extend stability at 4°C and 25°C are currently underway in our laboratories.

MATERIALS AND METHODS

Materials

Dulbecco's phosphate buffer solution (DPBS), Trizma base [2-amino-2-(hydroxymethyl)-1,3-propanediol] (Tris), PVA, Pluronic F127, sucrose, and trehalose were purchased from Sigma-Aldrich (St. Louis, MO). Glycerol (United States Pharmacopeia grade), and Aqualine Complete 5 solvent were purchased from Thermo Fisher Scientific Chemicals (Fair lawn, NJ). Dulbecco's modified Eagle's medium (DMEM), penicillin (10,000 IU) and streptomycin (10,000 µg/mL), and 0.25% trypsin EDTA sterile solution were purchased from Mediatech (Manassas, VA). Pluronic F68 was purchased from Gibco Life Technologies (Grand Island, NY). Fetal bovine serum was purchased from Mediatech (Corning, Woodlands, CA). Hydranal Formamide Dry was purchased from Honeywell (Charlotte, NC). Methanol, 99.8% extra dry, was provided from Acros Organics (Fair Lawn, NJ). Pullulan was obtained from TCI chemicals (Tokyo, Japan). Gelatin powder type A, 300 bloom, was purchased from Electron Microscopy Sciences (Hatfield, Pennsylvania). Compounds DMPE-PEG (Sunbright PM-020CN), DMG-PEG, and DMPC were purchased from NOF America (White Plains, NY) and Avanti Polar Lipids (Alabaster, AL), respectively. Polyethyleneimine (Linear, MW 25000, transfection grade) was purchased from Polysciences (Warrington, PA). Lipofectamine 2000 CD was purchased from Thermo Fisher Scientific Baltics (Vilnius, Lithuania). All other chemicals were of analytical reagent grade and purchased from Thermo Fisher Scientific (Pittsburgh, PA) unless specified otherwise.

Plasmid preparation

Transfection-grade plasmid (pAAV-LacZ, AAV Helper-Free System Stratagene, La Jolla, CA) was amplified in *Escherichia coli* (HB101 Competent cells, Promega, Madison, WI) and purified using Qiagen Maxi Plasmid kits (Qiagen, Germany). Plasmid stock (optical density [OD] 260/280 ratio 1.7–1.9) was diluted to a concentration of 1–2 mg/mL with 10 mM Tris buffer, pH 8, and stored at -20°C .

Preparation and storage of films containing plasmid complexes

PEI-DNA complexes were formed by adding 25 µg of pAAV-LacZ in 400 µL of medium to 100 µg of PEI in 400 µL of medium. Lipofectamine (LPF)-DNA complexes were formed by adding 20 µg of pAAV-LacZ in 250 µL (total volume) of Opti-Pro SFM medium (Gibco, Thermo Fisher Scientific) to 20 µL of LPF in 250 µL (total volume) of Opti-Pro SFM medium. Samples remained at RT for 20 min. At this time, 800-µL solutions containing PEI-DNA complexes were mixed with 200 µL of film formulation for a final DNA concentration of 25 µg/mL. Solutions containing LPF-DNA complexes were mixed with film formulation at a v/v ratio of 1:1 for a final DNA concentration of 20 µg/mL. The resulting solutions were dispensed into 100-µL silicon molds (Bold Maker, Amesbury, MA). All films were dried under aseptic conditions at 20°C . When drying was complete, a subset of films were reconstituted in transfection medium for analysis of loss due to drying. Remaining films were peeled and placed in Ziploc-like particle-free bags (American Cleanstat, Irvine, CA) inside a heat-sealed foil bag (Ted Pella, Redding, CA). For most stability studies summarized here, packaged films were stored in stability cham-

bers (Binder, Tuttlingen, Germany) set at 25°C , 60% RH, or at 4°C , 40%–50% RH. Details of each formulation are summarized in [Table S1](#).

Transfection (plasmid)

HEK293 cells (CRL-1573, ATCC, Manassas, VA, passage 12–26) were seeded in 12-well plates (Falcon, Corning, Durham, NC) at a density of 7×10^5 cells/well. When they were 80% confluent, culture medium was changed. One hour later, plasmid (1 µg) in 50 µL of Opti-MEM (Life Technologies, Grand Island, NY) was mixed with 4 µg of PEI in 50 µL of Opti-MEM. The resulting solution was incubated at RT for 20 min prior to addition to cells. For LPF-mediated transfection, plasmid (1 µg) in 12.5 µL of Opti-Pro was mixed well with 1 µL of LPF in 12.5 µL of Opti-Pro before dilution to a concentration of 1 µg of pAAV-LacZ/100 µL of medium per well. Rehydrated films were diluted to a final concentration of 1 µg/100 µL for transfection assays. Cells were then incubated at 37°C , 5% CO_2 , and culture medium replaced every 24 h. Forty-eight hours after transfection, cells were harvested for assessment of transgene expression.

Transfection efficiency (plasmid)

Analysis of beta-galactosidase expression was performed using a colorimetric assay based on an enzyme-mediated reaction with *ortho*-nitrophenyl-β-galactoside (ONPG). At the time of harvest, cells were washed with PBS prior to treatment with Reporter Lysis buffer (Promega, Madison, WI). After a freeze/thaw cycle and centrifugation at 14,000 rpm for 1 min, 10 µL of diluted supernatant was mixed with 150 µL of 14.3 M β-mercaptoethanol in 100 mM phosphate buffer at pH 7.5 and held at 37°C , 5% CO_2 , for 5 min. At that time, 50 µL of 4 mg/mL ONPG stock was added to the sample. After 2.5 min, color development was stopped by adding 90 µL of 1 M Na_2CO_3 . Absorbance at 420 nm for each sample was recorded. Transfection efficiency is expressed as the amount beta-galactosidase present per milligram of cell protein in a given cell population for each formulation with respect to cells transfected with freshly made PEI-DNA or LPF-DNA complexes prepared from plasmid stored frozen in Tris (pH 8).

Preparation and storage of films containing mRNA LNPs

LNPs, generously supplied by Greenlight Biosciences, were prepared by a proprietary manufacturing process, concentrated (1.5×) and sterile filtered prior to storage and shipment at $\leq -65^{\circ}\text{C}$. Prior to storage, the preparation was tested for critical attributes that are summarized in [Figure S3](#). On the day of film preparation, an aliquot of this stock (in 10% sucrose/Tris buffer, pH 8) was diluted to a concentration of 0.4 mg mRNA per milliliter. Note that reported LNP concentrations in this paper refer to mRNA concentrations. Bulk film formulations were prepared by first adding PEG lipids (4% stock in water) to 10 mM Tris buffer. Then, a volume of mRNA LNP stock equivalent to 25% of the total bulk formulation volume was added and gently mixed three times. Surfactants, if used in a formulation, were added to the resulting solution with gentle mixing. A mixture of polymer base prepared in 10 mM Tris buffer and glycerol (100%, USP grade) was incorporated last so that the final LNP concentration was 0.1 mg/mL. The final mixture was dispensed into 100-µL silicone molds using

an E3 Repeater pipette (Eppendorf, Hauppauge, NY) and dried under constant airflow, ambient ($20^{\circ}\text{C} \pm 1.5^{\circ}\text{C}$, 1 atm, 52.5% RH), and aseptic conditions. Temperature and humidity were monitored during the film-forming process with an Ambient Weather WS-3000-X5 Wireless Thermo-Hygrometer (Chandler, AZ). Once dry, films were peeled and rehydrated in 100- μL sterile Tris buffer pH 8 for 10 min at RT before gently mixing 10 times to ensure solutions were homogeneous. The resulting solution was then diluted 20-fold in PBS for transfection, 40-fold in nuclease-free Tris-EDTA for encapsulation efficiency, and 500-fold in $0.1\times$ PBS for dynamic light-scattering assays.

Physical characterization of LNPs: Dynamic light scattering

Samples were placed in cuvettes and hydrodynamic particle size measured at 25°C and a 173° backscatter angle using a Zetasizer ZS90 instrument (Malvern Instruments, Worcestershire, UK). Parameters were set for a particle refractive index of 1.45, absorption of 0.001, diluent viscosity of 0.888 cP, and refractive index of 1.335. Data were analyzed with Malvern Zetasizer Software version 8.00.4813.

Encapsulation efficiency

Quant-it RiboGreen Assay kits were utilized to determine encapsulation efficiency of LNPs in stock and various formulations (Thermo Fisher Scientific, Eugene, OR). The total amount of mRNA in a sample was determined by treating an aliquot of that sample with 0.5% Triton X-100 for 14 min. The RiboGreen reagent was added to all samples and fluorescence intensity (excitation at 480 nm and emission at 520 nm) measured 5 min later. Total and free mRNA concentrations in each sample were calculated using a mRNA standard curve in the range of 15–1,000 ng/mL. Encapsulation efficiency was determined based on the following equation.

$$\text{Encapsulation Efficiency (\%)} = \frac{\text{Total mRNA} - \text{Free mRNA}}{\text{Total mRNA}} \times 100$$

Transfection efficiency (mRNA LNP)

H1 HeLa cells (ATCC CRL-1958, passage 6–30) were seeded in 96-well plates (Thermo Fisher Scientific, Waltham, MA) at a density of 2×10^4 cells/well. Twenty-four hours later, medium was replaced an hour before samples containing mRNA LNPs equivalent to 50 ng of mRNA were added to each well. Twenty-four hours later, culture medium was replaced with 100 μL of Glo Lysis Buffer (Promega, Madison, WI) and luciferase expression measured using the Pierce Firefly Luc One-Step Glow Assay Kit (Thermo Fisher, Rockford, IL) according to the manufacturer's instructions. A portion of the lysate was also used to determine the protein content in each sample by Pierce BCA Protein assay kit (Thermo Fisher, Rockford, IL). Transgene expression in each sample was reported as RLU/mg protein and transfection efficiency calculated using the following equation:

$$\text{Transfection Efficiency} = \frac{\text{RLU sample}/C_{\text{protein sample}}}{\text{RLU control}/C_{\text{protein control}}} \times 100$$

Rheology

Viscosity of formulations was measured using an LVDV Brookfield viscometer (Brookfield AMETEK, Middleboro, MA). The cylinder sample adapter spindle (SC4-21) was lowered into the sample chamber (SC4-13R) filled with 8 g of formulation. The spindle was rotated at 20 rpm and torque (%) and viscosity (cP) recorded.

Residual moisture

Films were completely dissolved in 1 mL of extraction solvent (1:1 v/v ratio anhydrous formamide to extra-dry methanol) at 50°C and residual moisture determined as described previously.^{23,24}

Statistical analysis

Statistical analysis of data was conducted using Prism software (GraphPad Prism v.10.2.1, San Diego, CA).

DATA AND CODE AVAILABILITY

The authors agree that all reasonable requests for data and materials utilized in the studies summarized in this manuscript will be fulfilled and will require establishment of a materials transfer and/or license agreement between interested parties and the University of Texas at Austin, Jurata Thin Film, and/or Greenlight Biosciences.

SUPPLEMENTAL INFORMATION

Supplemental information can be found online at <https://doi.org/10.1016/j.omtn.2024.102179>.

ACKNOWLEDGMENTS

The authors thank the Dow Chemical Company (Midland, MI) and GreenLight Biosciences (Lexington, MA) for generously supplying the hydroxypropyl methyl cellulose-based polymers and the luciferase mRNA LNP stock utilized in these studies. We also thank Stephen C. Schafer for assistance with the design of Figure S1. This project was supported by a Sponsored Research Agreement from Jurata Thin Film (M.A.C.), The University of Texas at Austin Graduate School Writing and Continuing Fellowships (T.N.K.D.) and Endowed Graduate Fellowships from The University of Texas at Austin College of Pharmacy (T.N.K.D., M.M.D.).

AUTHOR CONTRIBUTIONS

T.N.K.D. participated in the design of experiments, assay development, collection and analysis of data collected from *in vitro* and *in vivo* studies, figure preparation, and writing of the manuscript. M.M.D. participated in data collection and analysis and editing of the final manuscript. M.A.C. oversaw study design and participated in data analysis and writing of the manuscript.

DECLARATION OF INTERESTS

M.A.C. serves as co-founder of and scientific advisor for Jurata Thin Film and holds several patents on film-based stabilization technology and equity in Jurata Thin Film. An international patent application (PCT/US2023/075045) has been filed related to this work.

REFERENCES

- Hou, X., Zaks, T., Langer, R., and Dong, Y. (2021). Lipid nanoparticles for mRNA delivery. *Nat. Rev. Mater.* 6, 1078–1094. <https://doi.org/10.1038/s41578-021-00358-0>.
- Guerrini, G., Gioria, S., Sauer, A.V., Lucchesi, S., Montagnani, F., Pastore, G., Ciabattini, A., Medaglini, D., and Calzolari, L. (2022). Monitoring Anti-PEG Antibodies Level upon Repeated Lipid Nanoparticle-Based COVID-19 Vaccine Administration. *Int. J. Mol. Sci.* 23, 8838. <https://doi.org/10.3390/ijms23168838>.
- Pacouret, S., Bouzelha, M., Shelke, R., Andres-Mateos, E., Xiao, R., Maurer, A., Mevel, M., Turunen, H., Barungi, T., Penaud-Budloo, M., et al. (2017). AAV-ID: A Rapid and Robust Assay for Batch-to-Batch Consistency Evaluation of AAV Preparations. *Mol. Ther.* 25, 1375–1386. <https://doi.org/10.1016/j.ymthe.2017.04.001>.
- Qin, S., Tang, X., Chen, Y., Chen, K., Fan, N., Xiao, W., Zheng, Q., Li, G., Teng, Y., Wu, M., and Song, X. (2022). mRNA-based therapeutics: powerful and versatile tools to combat diseases. *Signal Transduct. Targeted Ther.* 7, 166. <https://doi.org/10.1038/s41392-022-01007-w>.
- Tam, Y.Y.C., Chen, S., and Cullis, P.R. (2013). Advances in lipid nanoparticles for siRNA delivery. *Pharmaceutics* 5, 498–507. <https://doi.org/10.3390/pharmaceutics5030498>.
- Han, X., Zhang, H., Butowska, K., Swingle, K.L., Alameh, M.-G., Weissman, D., and Mitchell, M.J. (2021). An ionizable lipid toolbox for RNA delivery. *Nat. Commun.* 12, 7233. <https://doi.org/10.1038/s41467-021-27493-0>.
- Sfera, A., Hazan, S., Anton, J.J., Sfera, D.O., Andronescu, C.V., Sasannia, S., Rahman, L., and Kozlakidis, Z. (2022). Psychotropic drugs interaction with the lipid nanoparticle of COVID-19 mRNA therapeutics. *Front. Pharmacol.* 13, 995481. <https://doi.org/10.3389/fphar.2022.995481>.
- Boafo, G.F., Magar, K.T., Ekpo, M.D., Qian, W., Tan, S., and Chen, C. (2022). The Role of Cryoprotective Agents in Liposome Stabilization and Preservation. *Int. J. Mol. Sci.* 23, 12487. <https://doi.org/10.3390/ijms232012487>.
- Zhang, H., Leal, J., Soto, M.R., Smyth, H.D.C., and Ghosh, D. (2020). Aerosolizable Lipid Nanoparticles for Pulmonary Delivery of mRNA through Design of Experiments. *Pharmaceutics* 12, 1042. <https://doi.org/10.3390/pharmaceutics12111042>.
- Yanez Arteta, M., Kjellman, T., Bartesaghi, S., Wallin, S., Wu, X., Kvist, A.J., Dabkowska, A., Székely, N., Radulescu, A., Bergenholtz, J., and Lindfors, L. (2018). Successful reprogramming of cellular protein production through mRNA delivered by functionalized lipid nanoparticles. *Proc. Natl. Acad. Sci. USA* 115, E3351–E3360. <https://doi.org/10.1073/pnas.1720542115>.
- Klimek, L., Novak, N., Cabanillas, B., Jutel, M., Bousquet, J., and Akdis, C.A. (2021). Allergenic components of the mRNA-1273 vaccine for COVID-19: Possible involvement of polyethylene glycol and IgG-mediated complement activation. *Allergy* 76, 3307–3313. <https://doi.org/10.1111/all.14794>.
- Cullis, P.R., and Hope, M.J. (2017). Lipid Nanoparticle Systems for Enabling Gene Therapies. *Mol. Ther.* 25, 1467–1475. <https://doi.org/10.1016/j.ymthe.2017.03.013>.
- Li, S., Hu, Y., Li, A., Lin, J., Hsieh, K., Schneiderman, Z., Zhang, P., Zhu, Y., Qiu, C., Kokkoli, E., et al. (2022). Payload distribution and capacity of mRNA lipid nanoparticles. *Nat. Commun.* 13, 5561. <https://doi.org/10.1038/s41467-022-33157-4>.
- Kim, B., Hosn, R.R., Remba, T., Yun, D., Li, N., Abraham, W., Melo, M.B., Cortes, M., Li, B., Zhang, Y., et al. (2023). Optimization of storage conditions for lipid nanoparticle-formulated self-replicating RNA vaccines. *J. Control Release.* 353, 241–253. <https://doi.org/10.1016/j.jconrel.2022.11.022>.
- Oude Blenke, E., Örnkvist, E., Schöneich, C., Nilsson, G.A., Volkin, D.B., Mastrobattista, E., Almarsson, Ö., and Crommelin, D.J.A. (2023). The Storage and In-Use Stability of mRNA Vaccines and Therapeutics: Not A Cold Case. *J. Pharmaceut. Sci.* 112, 386–403. <https://doi.org/10.1016/j.xphs.2022.11.001>.
- Schoenmaker, L., Witzigmann, D., Kulkarni, J.A., Verbeke, R., Kersten, G., Jiskoot, W., and Crommelin, D.J.A. (2021). mRNA-lipid nanoparticle COVID-19 vaccines: Structure and stability. *Int. J. Pharm.* 601, 120586. <https://doi.org/10.1016/j.ijpharm.2021.120586>.
- (2022). Moderna COVID-19 Vaccine: Storage and Handling Summary (CDC). <https://www.cdc.gov/vaccines/covid-19/info-by-product/moderna/downloads/storage-summary.pdf>.
- (2022). Pfizer-BioNTech COVID-19 Vaccine: Storage and Handling Summary (CDC). <https://www.cdc.gov/vaccines/covid-19/info-by-product/pfizer/downloads/storage-summary.pdf>.
- Muramatsu, H., Lam, K., Bajusz, C., Laczkó, D., Karikó, K., Schreiner, P., Martin, A., Lutwyche, P., Heyes, J., and Pardi, N. (2022). Lyophilization provides long-term stability for a lipid nanoparticle-formulated, nucleoside-modified mRNA vaccine. *Mol. Ther.* 30, 1941–1951. <https://doi.org/10.1016/j.ymthe.2022.02.001>.
- Ai, L., Li, Y., Zhou, L., Yao, W., Zhang, H., Hu, Z., Han, J., Wang, W., Wu, J., Xu, P., et al. (2023). Lyophilized mRNA-lipid nanoparticle vaccines with long-term stability and high antigenicity against SARS-CoV-2. *Cell Discov.* 9, 9. <https://doi.org/10.1038/s41421-022-00517-9>.
- Czyż, M.P. (2016). Thermostability of Freeze-Dried Plant-Made VLP-Based Vaccines. In *Sustainable Drying Technologies*, J. Del Real Olvera, ed. (IntechOpen), pp. 7–36. <https://doi.org/10.5772/63503>.
- Bajrovic, I., Schafer, S.C., Romanovic, D.K., and Croyle, M.A. (2020). Novel technology for storage and distribution of live vaccines and other biological medicines at ambient temperature. *Sci. Adv.* 6, eaau4819. <https://doi.org/10.1126/sciadv.aau4819>.
- Doan, T.N.K., Le, M.D., Bajrovic, I., Celentano, L., Krause, C., Balyan, H.G., Svancarek, A., Mote, A., Tretiakova, A., Jude Samulski, R., and Croyle, M.A. (2022). Thermostability and in vivo performance of AAV9 in a film matrix. *Commun. Med.* 2, 148. <https://doi.org/10.1038/s43856-022-00212-6>.
- Kieu Doan, T.N., and Croyle, M.A. (2023). Physical characteristics and stability profile of recombinant plasmid DNA within a film matrix. *Eur. J. Pharm. Biopharm.* 190, 270–283. <https://doi.org/10.1016/j.ejpb.2023.08.005>.
- Yang, S., Zhou, X., Li, R., Fu, X., and Sun, P. (2017). Optimized PEI-based Transfection Method for Transient Transfection and Lentiviral Production. *Curr. Protoc. Chem. Biol.* 9, 147–157. <https://doi.org/10.1002/cpch.25>.
- Cardarelli, F., Digiacomo, L., Marchini, C., Amici, A., Salomone, F., Fiume, G., Rossetta, A., Grattón, E., Pozzi, D., and Caracciolo, G. (2016). The intracellular trafficking mechanism of Lipofectamine-based transfection reagents and its implication for gene delivery. *Sci. Rep.* 6, 25879. <https://doi.org/10.1038/srep25879>.
- Bajrovic, I., Le, M.D., Davis, M.M., and Croyle, M.A. (2022). Evaluation of intermolecular interactions required for thermostability of a recombinant adenovirus within a film matrix. *J. Control Release* 341, 118–131. <https://doi.org/10.1016/j.jconrel.2021.11.012>.
- Tharmalingam, T., and Goudar, C.T. (2015). Evaluating the impact of high Pluronic® F68 concentrations on antibody producing CHO cell lines. *Biotechnol. Bioeng.* 112, 832–837. <https://doi.org/10.1002/bit.25491>.
- Kerwin, B.A. (2008). Polysorbates 20 and 80 used in the formulation of protein biotherapeutics: structure and degradation pathways. *J. Pharmaceut. Sci.* 97, 2924–2935. <https://doi.org/10.1002/jps.21190>.
- Kamiya, M., Matsumoto, M., Yamashita, K., Izumi, T., Kawaguchi, M., Mizukami, S., Tsurumaru, M., Mukai, H., and Kawakami, S. (2022). Stability Study of mRNA-Lipid Nanoparticles Exposed to Various Conditions Based on the Evaluation between Physicochemical Properties and Their Relation with Protein Expression Ability. *Pharmaceutics* 14, 2357. <https://doi.org/10.3390/pharmaceutics14112357>.
- Liu, T., Tian, Y., Zheng, A., and Cui, C. (2022). Design Strategies for and Stability of mRNA-Lipid Nanoparticle COVID-19 Vaccines. *Polymers* 14, 4195. <https://doi.org/10.3390/polym14194195>.
- Packer, M., Gyawali, D., Yerabolu, R., Schariter, J., and White, P. (2021). A novel mechanism for the loss of mRNA activity in lipid nanoparticle delivery systems. *Nat. Commun.* 12, 6777. <https://doi.org/10.1038/s41467-021-26926-0>.
- Ghadermazi, R., Hamdipour, S., Sadeghi, K., Ghadermazi, R., and Khosrowshahi Asl, A. (2019). Effect of various additives on the properties of the films and coatings derived from hydroxypropyl methylcellulose-A review. *Food Sci. Nutr.* 7, 3363–3377. <https://doi.org/10.1002/fsn3.1206>.
- Olechno, K., Basa, A., and Winnicka, K. (2021). “Success Depends on Your Backbone”—About the Use of Polymers as Essential Materials Forming Orodispersible Films. *Materials* 14, 4872. <https://doi.org/10.3390/ma14174872>.
- Panraksa, P., Udomsom, S., Rachtanapun, P., Chittasupho, C., Ruksiriwanich, W., and Jantrawut, P. (2020). Hydroxypropyl Methylcellulose E15: A Hydrophilic Polymer for Fabrication of Orodispersible Film Using Syringe Extrusion 3D Printer. *Polymers* 12, 2666. <https://doi.org/10.3390/polym12112666>.

36. Krull, S.M., Ammirata, J., Bawa, S., Li, M., Bilgili, E., and Davé, R.N. (2017). Critical Material Attributes of Strip Films Loaded With Poorly Water-Soluble Drug Nanoparticles: II. Impact of Polymer Molecular Weight. *J. Pharmaceut. Sci.* *106*, 619–628. <https://doi.org/10.1016/j.xphs.2016.10.009>.
37. Otoni, C.G., Lorevice, M.V., Moura, M.R.d., and Mattoso, L.H.C. (2018). On the effects of hydroxyl substitution degree and molecular weight on mechanical and water barrier properties of hydroxypropyl methylcellulose films. *Carbohydr. Polym.* *185*, 105–111. <https://doi.org/10.1016/j.carbpol.2018.01.016>.
38. Hassett, K.J., Higgins, J., Woods, A., Levy, B., Xia, Y., Hsiao, C.J., Acosta, E., Almarsson, Ö., Moore, M.J., and Brito, L.A. (2021). Impact of lipid nanoparticle size on mRNA vaccine immunogenicity. *J. Contr. Release* *335*, 237–246. <https://doi.org/10.1016/j.jconrel.2021.05.021>.
39. Duong, V.-A., Nguyen, T.-T.-L., and Maeng, H.-J. (2020). Preparation of Solid Lipid Nanoparticles and Nanostructured Lipid Carriers for Drug Delivery and the Effects of Preparation Parameters of Solvent Injection Method. *Molecules* *25*, 4781. <https://doi.org/10.3390/molecules25204781>.
40. Bajrovic, I., Le, M.D., Davis, M.M., and Croyle, M.A. (2022). Evaluation of intermolecular interactions required for thermostability of a recombinant adenovirus within a film matrix. *J. Contr. Release* *341*, 118–131. <https://doi.org/10.1016/j.jconrel.2021.11.012>.
41. Spark Therapeutics Inc (2017). Luxterna (voretigene neparovec-rzyl) [Package Insert].
42. Novartis Gene Therapies Inc (2021). Zolgensma (onasemnogene abeparovec-xioi) [Package Insert].
43. Bąk, A., Pilarek, M., Podgórska, W., Markowska-Radomska, A., and Hubacz, R. (2018). Surface properties of perfluorodecalin-containing liquid/liquid systems: The influence of Pluronic F-68 dissolved in the aqueous phase. *J. Fluor. Chem.* *215*, 36–43. <https://doi.org/10.1016/j.jfluchem.2018.09.002>.
44. Song, Y., Tian, Q., Huang, Z., Fan, D., She, Z., Liu, X., Cheng, X., Yu, B., and Deng, Y. (2014). Self-assembled micelles of novel amphiphilic copolymer cholesterol-coupled F68 containing cabazitaxel as a drug delivery system. *Int. J. Nanomed.* *9*, 2307–2317. <https://doi.org/10.2147/IJN.S61220>.
45. Zhang, P.-Q., Tan, P.-C., Gao, Y.-M., Zhang, X.-J., Xie, Y., Zheng, D.-N., Zhou, S.-B., and Li, Q.-F. (2022). The effect of glycerol as a cryoprotective agent in the cryopreservation of adipose tissue. *Stem Cell Res. Ther.* *13*, 152. <https://doi.org/10.1186/s13287-022-02817-z>.
46. Larson, N.R., Hu, G., Wei, Y., Tuesca, A.D., Forrest, M.L., and Middaugh, C.R. (2022). pH-Dependent Phase Behavior and Stability of Cationic Lipid-mRNA Nanoparticles. *J. Pharmaceut. Sci.* *111*, 690–698. <https://doi.org/10.1016/j.xphs.2021.11.004>.
47. Doan, L.P., Dao, N.G., Nguyen, D.C., Dang, T.H.T., Vu, G.T., Nguyen, L.H., Vu, L.G., Le, H.T., Latkin, C.A., Ho, C.S.H., and Ho, R.C.M. (2023). Having Vaccines is Good But Not Enough: Requirements for Optimal COVID-19 Immunization Program in Vietnam. *Front. Public Health* *11*, 1137401. <https://doi.org/10.3389/fpubh.2023.1137401>.
48. Warne, N., Ruesch, M., Siwik, P., Mensah, P., Ludwig, J., Hripcsak, M., Godavarti, R., Prigodich, A., and Dolsten, M. (2023). Delivering 3 Billion Doses of COMIRNATY in 2021. *Nat. Biotechnol.* *41*, 183–188. <https://doi.org/10.1038/s41587-022-01643-1>.
49. Hanson, C.M., George, A.M., Sawadogo, A., and Schreiber, B. (2017). Is Freezing in the Vaccine Cold Chain An Ongoing Issue? A Literature Review. *Vaccine* *35*, 2127–2133. <https://doi.org/10.1016/j.vaccine.2016.09.070>.